IR spectroscopy of adsorbed NO as a useful tool for the characterisation of low concentrated Fe-silicalite catalysts

G. Berlier*, G. Spoto, G. Ricchiardi, S. Bordiga, C. Lamberti, A. Zecchina

Dipartimento di Chimica I.F.M., Università di Torino, Via P. Giuria 7, I-10125 Torino, Italy

Abstract

FT-IR spectroscopy of adsorbed NO was used to investigate the electronic and geometric structure of the extraframework iron species formed upon thermal activation of four Fe-silicalite samples with Si/Fe ratios ranging from 25 to 150. An heterogeneous family of grafted Fe^{2+} species, classified in terms of their first coordination shell, i.e. as $L_2N_nFe^{2+}$ (where L are the framework SiO^- groups chemically linked to the Fe species and N are the framework oxygen atoms of the vicinal Si–O–Si bridges interacting with Fe centres via electrostatic forces) has been detected as the primary product of the Fe migration. Depending upon the number of N ligands (3, 2 or 1) the Fe^{2+} species can adsorb one, two, and three NO molecules, respectively, with formation of well-defined nitrosylic complexes. $L_2N_nFe^{2+}$ ($n = 1$ and 2) are supposed to be isolated species, while $L_2N_3Fe^{2+}$ are probably dimeric or polymeric clusters. Fe^{3+} extraframework species can be reduced to Fe^{2+} by prolonged outgassing in vacuo. The formation of large Fe_2O_3 clusters is inferred for the most concentrated sample. O_2 dissociates with formation of adsorbed oxygen on all extraframework Fe species at 573 K. At room temperature only dimeric or polymeric $L_2N_3Fe^{2+}$ species are able to dissociate O_2. © 2002 Elsevier Science B.V. All rights reserved.

Keywords: Fe-silicalite; Nitrosylic complexes; Extraframework species; FT-IR

1. Introduction

Fe-containing zeolites have been deeply studied in the 1970s because of their remarkable redox behaviour [1–6]. In more recent years, these redox systems have attracted new interest from both the industrial and the academic point of view, because it was discovered that Fe-MFI zeolites (Fe-silicalite and Fe-ZSM-5) are active in partial oxidation reactions. The oxidation of benzene to phenol, using N_2O as oxidising agent, is in fact a promising process for the phenol manufactory, being a one-step process with no side products or dangerous reaction inter-

mediate (as it is for the actually employed cumene process) [7–10]. The interest for Fe-silicalite and Fe-ZSM-5 is also reinforced by the observation that Fe-ZSM-5 is active in the oxidation of methane to methanol at room temperature [11,12], a fact that makes it resembling to the MMO enzyme [13,14]. The possibility of developing an inorganic biomimetic catalyst capable of activating oxygen analogous to MMO has obviously fascinated a large number of researcher.

Zeolites can be considered as nanometre-scale reactors, where isolated redox sites, dispersed in the narrow zeolite channels and cavities, can play their redox activity with high selectivity [15]. The introduction of metallic ions in the zeolitic channels is usually obtained by post-synthesis exchange. On the contrary,

* Corresponding author. Fax: +39-11-6707855.
E-mail address: berlier@ch.unito.it (G. Berlier).

in Fe-MFI systems, iron is introduced during the synthesis into the zeolitic framework, as isolated Fe^{3+} tetrahedral species. Extraframework iron species, highly dispersed into the zeolitic channels and cavities, are only obtained by post-synthesis treatments consisting in thermal activation of the catalyst at high temperature. In fact, thermal treatments favouring the breaking of zeolitic Si–O–Fe bonds allow the migration of iron into extraframework positions [16–21]. The extraframework species formed in this way are able to decompose N_2O to give an adsorbed, highly reactive oxygen species, able to selectively attack the hydrocarbons [22–25].

The structure of the extraframework Fe species has been the subject of many investigations; however, till now no definite conclusions have been obtained. On the basis of quantum calculations Filatov et al. [26] have hypothesised that the active sites are dimeric iron clusters, similar to that reported for MMO [14]. More recently, a model structure containing an isolated Fe^+ centre has been suggested by Yoshizawa et al. [27]. Both structures are hypothetical and are not based on well-established experimental data. It is a matter of fact that the characterisation of Fe extraframework centres in Fe-MFI materials is complicated by two main problems. The first problem is related to the low iron concentration of the active catalysts [28,29]. This low concentration makes most of the classical techniques inapplicable. The second problem is related to the intrinsic complexity of the system, because the species which can be formed upon the iron migration from framework to extraframework positions can be very numerous and their relative concentration is strictly dependent upon the activation conditions. In particular the presence of oxidising or reducing agents (such as water traces or unavoidable carbonaceous impurities) can tune the oxidation state of iron among Fe^{2+}, Fe^{3+} or Fe^{4+}. Furthermore, as extraframework iron can be present as isolated, dimeric or larger clusters, all these factors taken together can lead to highly heterogeneous systems, where more than one Fe species is present. For this reason, in this study we report about a new investigation based on the IR spectroscopy of adsorbed NO, which, forming stable and highly IR active complexes with iron species, give unprecedented information about iron structure in very diluted samples, closely resembling the real active catalysts.

2. Experimental

Four different Fe-silicalite samples, characterised by a Si/Fe ratio of 25, 50, 90 and 150 (hereafter named as FeS25, FeS50, FeS90 and FeS150, respectively) have been studied. Concerning the synthesis, samples FeS25, FeS50, and FeS150 have been prepared following the method of Szostak [30] while for FeS90 the hydrothermal method described by Ratnasamy and Kumar [31] has been adopted.

The IR experiments were carried out on a Bruker IFS 66 FT-IR instrument equipped with a cryogenic MCT detector and running at $2\,cm^{-1}$ resolution. The Fe-silicalite samples were in the form of self-supporting pellets suitable for measurements in transmission mode. Measurement cells, allowing in situ thermal treatments (in vacuo and with O_2), IR measurements and dosing of NO were used. Burning or decomposition of the template was performed either in air at 773 K ($0.5\,°C/min$ up to 393 K, $1\,°C/min$ up to 773 K) or under vacuo at the same temperature ($3\,°C/min$). In the first case, as cooling the sample in air after removal of the template causes readsorption of water and other impurities, samples were carefully re-activated at 773 K under vacuo before NO dosage. The two procedures leaded to similar results. NO, carefully purified by distillation in order to remove other undesired nitrogen oxides, was dosed at room temperature (RT) to obtain the maximum coverage ($P_{NO} = 15\,Torr$). The other IR spectra were then recorded by gradually reducing the P_{NO}. The last spectrum typically corresponds to 15 min outgassing at RT (residual pressure lower than $10^{-3}\,Torr$). In all experiments, the IR spectrum collected before gas dosage was used as background. All reported spectra are background-subtracted.

3. Results and discussion

3.1. Formation of polynitrosylic complexes on extraframework ferrous species

The adsorption of NO at RT on Fe-silicalite samples originates bands in the $1950–1700\,cm^{-1}$ range. Although the obtained spectra are substantially reproducible, some variability is observed. In Fig. 1 two typical NO spectra ($P_{NO} = 15\,Torr$) obtained on
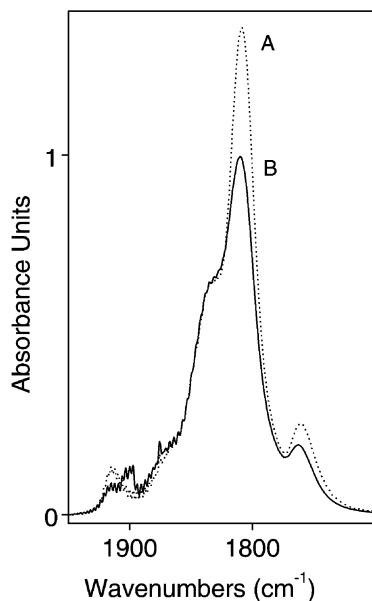
Fig. 1. IR spectra of NO dosed at RT ($P_{NO} = 15$ Torr) on sample FeS50 after activation in vacuo at 773 K for 2 h (dotted line, spectrum A) and for 1 h (solid line, spectrum B).

Fig. 2. IR spectra of NO dosed at RT (decreasing P_{NO} from 15 Torr (dotted line) spectrum to 10^{-3} Torr (dashed line) spectrum) on sample FeS90 after activation in vacuo at 773 K for 2 h.

samples apparently treated in the same way are compared. From this comparison and from the results obtained on different samples after different pre-activation time, we can conclude that spectrum A of Fig. 1 is favoured by prolonged activation or by reductive treatments in H_2, while spectrum B is typical of samples pre-treated in vacuo for less than 2 h. As Fe^{3+} centres in the framework positions are necessarily inactive towards interaction with d–π accepting ligands, the bands shown in Fig. 1 must be attributed to nitrosylic complexes formed on iron species in extraframework positions.

Fig. 2 illustrates the behaviour, upon pressure changes, of the nitrosylic bands obtained on a FeS90 sample previously activated at 773 K for 2 h. As a first observation, it is worth underlying the "molecular definition" of the spectra (in terms of half-width and symmetry) which reminds those of homogeneous complexes, where the isolated metallic centres are in a well-defined environment. Broader nitrosylic bands in the same spectral range have been already observed on pre-reduced silica-supported iron oxide [32] or Fe-containing zeolites [2,33–35] and were assigned to Fe^{2+} species. We fully agree with this interpretation.
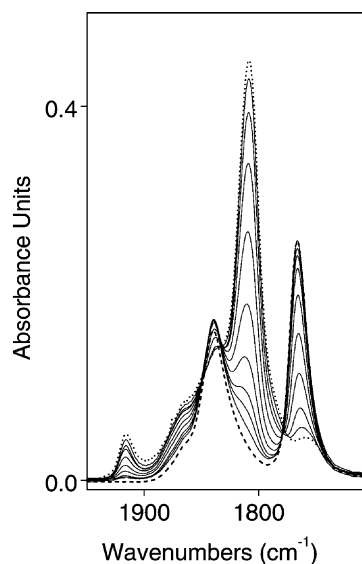
This implies that, during the migration of Fe^{3+} from the framework into extraframework positions, a reductive process has occurred. If this is due to spontaneous loss of oxygen at high temperature or to the action of unavoidable carbonaceous impurities (or both) it is for the moment hard to say.

Coming to a more detailed attribution of the nitrosylic bands, the first observation is that the spectra are mainly composed by two couples of bands: the first one, at 1916 and 1810 cm^{-1}, gradually decreases by reducing P_{NO}, while the second, at 1838 and 1765 cm^{-1}, grows and finally dominates the spectra after outgassing at RT. A large and broad adsorption (not totally disappearing upon reduction of P_{NO}) is also observed in the 1880–1850 cm^{-1} range. The conversion of the 1916 and 1810 cm^{-1} couple into the 1835 and 1765 cm^{-1} pair upon reducing P_{NO} is witnessed by three well-defined isosbestic points at 1850, 1830 and 1778 cm^{-1}. These spectroscopic manifestations have been assigned to the equilibrium [36]:

$$Fe^{2+}(NO)_2 \underset{-NO}{\overset{+NO}{\rightleftharpoons}} Fe^{2+}(NO)_3 \qquad (1)$$
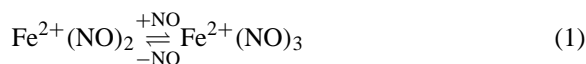
where the $Fe^{2+}(NO)_2$ complex is responsible for the couple of bands at 1838 and 1765 cm^{-1},

while $Fe^{2+}(NO)_3$ generates the bands at 1916 and 1810 cm^{-1}. This assignment has been confirmed by adsorption of an isotopic $^{14}NO/^{15}NO$ mixture [36]. The ability of these Fe^{2+} species to add up to three NO molecules, together with the sharpness and high definition of the nitrosylic bands strongly suggest that we are dealing with isolated coordinatively unsaturated Fe^{2+} species, probably grafted to the inner zeolite surface. The attribution of the large adsorption in the 1880–1850 cm^{-1} range is more troublesome and will not be commented anymore.

3.2. Effect of Si/Fe ratio on the structure of extraframework ferrous species

In Fig. 3 the IR spectra obtained upon adsorption of NO on four different samples with Si/Fe ratio ranging from 25 to 150 are reported. All samples have been activated in vacuo at 773 K for 2 h. For simplicity we only report the spectra obtained at high and low P_{NO} (Fig. 3a and b, respectively), while the spectra corresponding to intermediate coverage are omitted. First we underline that the intensity of the nitrosylic bands does not increase proportionally with the iron loading: this is particularly evident if we compare the spectra
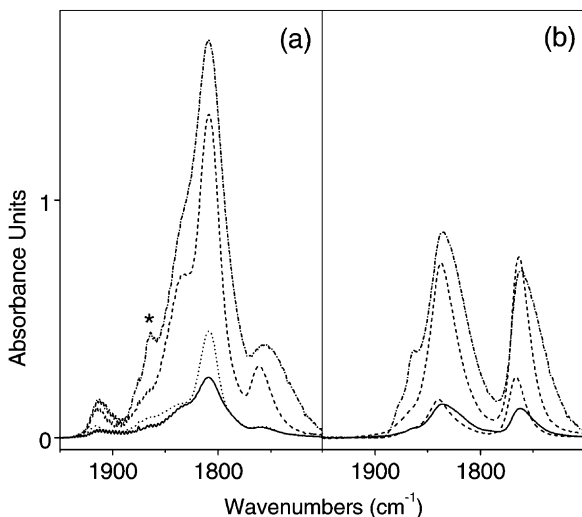

Fig. 3. IR spectra of NO dosed at RT on samples FeS150 (solid line), FeS90 (dotted line), FeS50 (dashed line) and FeS25 (dot-dashed line) after activation in vacuo at 773 K for 2 h. (a) The spectra obtained at $P_{NO} = 15$ Torr; (b) the spectra recorded after 15 min outgassing at RT ($P_{NO} < 10^{-3}$ Torr).

obtained on samples FeS50 and FeS25 in Fig. 3a (dashed and dot-dashed lines, respectively). This observation suggests that by increasing the iron loading an increasing fraction of iron becomes "invisible" to the NO probe, i.e. not all the iron atoms are well dispersed in accessible positions.
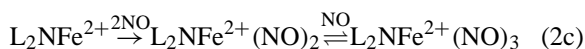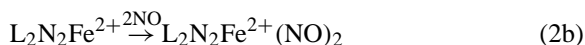
This phenomenon can be easily explained with the formation of small oxidic clusters, where most of iron atoms are not on the surface, and thus not able to interact with NO. This seems to be particularly true for the most concentrated sample (FeS25). In fact the Si/Fe = 25 ratio represents the lower limit to obtain Fe-silicalite samples with good iron dispersion, while higher iron concentration results in the formation of Fe_2O_3 aggregates during the synthesis [37,38]. We cannot thus exclude that the formation of Fe_2O_3 aggregates in the FeS25 sample has occurred before the thermal treatment.

As a consequence, the sharp band at 1865 cm^{-1} (indicated by a star in Fig. 3a) can be assigned to $Fe^{3+}(NO)$ complexes formed on the surface of small oxidic clusters. This band is only present on the most concentrated sample (FeS25) which, on the other hand, shows a light-brown colour characteristic of Fe_2O_3 nanoparticles. Furthermore, this assignment is supported by the fact that the same band has been observed on steamed samples, where large oxide clusters are certainly favoured [39].

The second observation regards the relative intensity of the single components. In particular, when the spectra at low P_{NO} are considered (Fig. 3b), it is emerging that the intensity ratio of the 1838 and 1765 cm^{-1} pair is not constant. As this couple of bands has been assigned [36,39] to the symmetric (ν_{sym}) and asymmetric (ν_{asym}) stretching modes, respectively, of a single $Fe^{2+}(NO)_2$ species (an assignment requiring a constant intensity ratio, with $I_{\nu_{asym}} > I_{\nu_{sym}}$) it is inferred that a second $Fe^{2+}(NO)$ species contributes to the absorption around 1835 cm^{-1}.

Coming back to the spectra reported in Fig. 3a we underline the fact that, under these conditions (high P_{NO}), the equilibrium reported in (1) should be strongly displaced towards the formation of $Fe^{2+}(NO)_3$ complexes. On the contrary it can be observed that, even at the highest NO coverage the band at 1765 cm^{-1} (assigned to $Fe^{2+}(NO)_2$ species) is not totally consumed. This indicates that a fraction of ferrous species, although able to form $Fe^{2+}(NO)_2$

complexes, cannot evolve towards trinitrosylic complexes. All these facts together lead to the conclusion that at least three different Fe^{2+} species are detectable by the NO probe, which differ upon the number of NO ligands they can take, as schematically illustrated in schemes (2a)–(2c):

$$L_2N_3Fe^{2+} \xrightarrow{NO} L_2N_3Fe^{2+}(NO) \quad (2a)$$

$$L_2N_2Fe^{2+} \xrightarrow{2NO} L_2N_2Fe^{2+}(NO)_2 \quad (2b)$$

$$L_2NFe^{2+} \xrightarrow{2NO} L_2NFe^{2+}(NO)_2 \xrightleftharpoons{NO} L_2NFe^{2+}(NO)_3 \quad (2c)$$

Schemes (2a)–(2c) have been drawn by assuming that the adsorption of NO ligands is saturating the pre-existing coordinative vacancy of Fe^{2+}. On this basis the three different species can be written as $L_2N_nFe^{2+}$, where L are the framework SiO^- groups chemically linked to the Fe species and N are the framework oxygen atoms of the vicinal Si–O–Si bridges interacting with Fe centres via electrostatic forces. In other words, although extraframework Fe^{2+} species are all chemically linked to the inner zeolitic surface by means of two equivalent SiO^- ligands, their local environment can be different depending upon their location on the zeolitic walls and channels, because of the presence of a number of vicinal Si–O–Si groups (N ligands) varying from 1 to 3. Depending upon the number of N ligands (3, 2 or 1), the Fe^{2+} species can adsorb one, two, and three NO molecules, respectively, with formation of well-defined mono-, di- and trinitrosylic species.

Some significant differences can be observed if we compare the nitrosylic bands obtained on the different samples. As a first approximation we can conclude that the concentration of the less coordinatively unsaturated $L_2N_3Fe^{2+}$ species (responsible for the formation of mononitrosylic complexes as depicted in scheme (2a)) is growing by increasing the iron content. Notice that in the low concentrated sample FeS90 these species are virtually absent, in fact the spectra of Fig. 2 have been assigned invoking only one Fe^{2+} species (see schemes (1) and (2c)). However, the same does not hold for the low concentrated sample FeS150, indicating that also the synthesis methods can play an important role in determining the iron dispersion [30,31].

In our previous work [36], where only sample FeS50 was considered, we were able to detect only two of the three Fe^{2+} species here discussed. There we were not able to completely understand the complexity of the nitrosylic bands and to propose a detailed hypothesis about the structure of extraframework species. We want to stress the fact that only the comparison of the results obtained on different samples allowed us to throw light on a very complex system, with the formulation of a structural notation, $L_2N_nFe^{2+}$, which is able to completely explain the great complexity of the nitrosylic bands.

3.3. Extraframework Fe^{3+} species

As mentioned in the comment of Fig. 1, samples outgassed for a short time tend to show preferentially the spectrum B of Fig. 1. In Fig. 4 we report in detail the IR spectra of NO adsorbed on a FeS50 sample activated at 773 K for 1 h only. By comparison with the spectra obtained on samples activated for 2 h or more, we notice a general diminution of the intensity of the bands assigned to $L_2N_nFe^{2+}$ nitrosylic complexes.
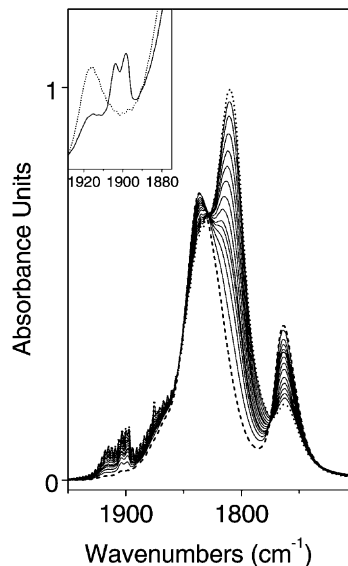

Fig. 4. IR spectra of NO dosed at RT (decreasing P_{NO} from 15 Torr (dotted line) spectrum to 10^{-3} Torr (dashed line) spectrum) on sample FeS50 after activation in vacuo at 773 K for 1 h. The inset reports the magnification in the region of $Fe^{3+}(NO)$ complexes of the $P_{NO} = 10^{-2}$ Torr spectrum (solid line) and of the comparable spectrum obtained on the catalyst reduced in H_2 (dotted line).

This is particularly true for the bands assigned to trinitrosylic complexes. Moreover, a new sharp doublet around $1900\,cm^{-1}$ is observed (an exploded view can be appreciated in the inset). The observed stretching frequency is higher than that of NO gas: this is the result of a reduced back-bond ability. As a consequence these new bands are assigned to NO adsorbed on two different Fe^{3+} centres. This assignment is also proved by the fact that the peaks at $\sim 1900\,cm^{-1}$ are absent on samples pre-reduced in hydrogen (dotted line in the inset).

This experiment indicates that, beside Fe^{2+}, also extraframework Fe^{3+} species must be considered. Fe^{2+} and Fe^{3+} extraframework species can be transformed into the others by changing the reducing conditions. In particular Fe^{3+} species can be reduced to $L_2N_nFe^{2+}$ by prolonged activation treatments in vacuo either because of spontaneous loss of oxygen or because of the action of carbonaceous impurities. In conclusion, the relative concentration of Fe^{2+} and Fe^{3+} species in diluted samples, characterised by $Si/Fe > 25$, is strictly depending upon the activation temperature and reducing impurities. For this reason the final oxidation state of Fe in very diluted samples cannot be easily controlled.

3.4. The effect of preadsorbed oxygen

In Fig. 5 we report the IR spectra of NO adsorbed on sample FeS50 previously treated with O_2 at RT (a) and at 573 K (b). By comparing the spectra of Fig. 5a with those reported in Fig. 4, some significant changes can be noticed. After the oxidising treatment at RT, the doublet at $1900\,cm^{-1}$ assigned to $Fe^{3+}(NO)$ complexes slightly increases, while the band at $1835\,cm^{-1}$, mainly due to $L_2N_3Fe^{2+}(NO)$ complexes is strongly depressed (as indicated by an arrow in Fig. 5a). The bands assigned to $L_2NFe^{2+}(NO)_3$ complexes are less affected, indicating that oxidation with O_2 of isolated ferrous sites is not occurring at RT. Dissociation of O_2 at RT is on the contrary occurring on $L_2N_3Fe^{2+}$ species. This result is surprising, because, being the $L_2N_3Fe^{2+}$ species less coordinatively unsaturated, they should be also less reactive. This difficulty is surmounted if we are dealing with clustered dimeric or polymeric species where O_2 is dissociated on couples of suitably located Fe^{2+} ions, with formation of O^{2-} and O_2^{2-} bridging species. Notice that adsorbed oxygen is gradually reacting with NO and that the products of this oxidation are observed in the 2150–$2100\,cm^{-1}$ range (see inset) [39].
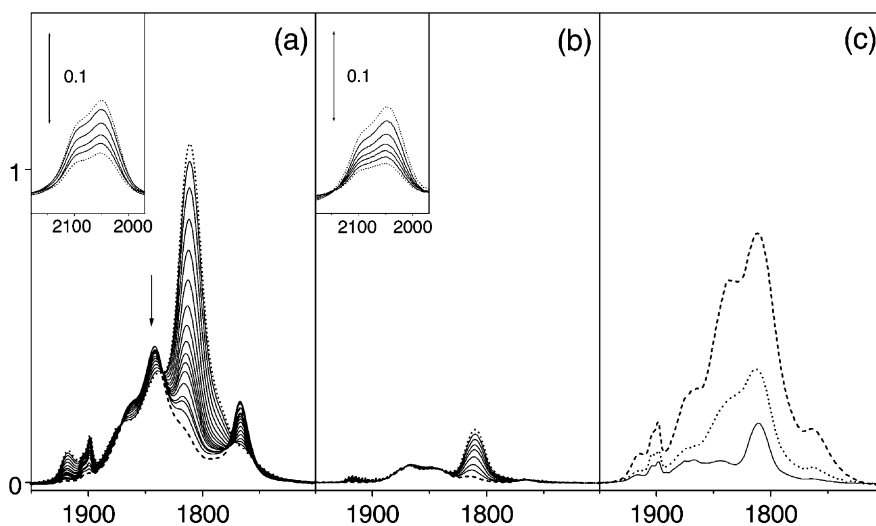

Fig. 5. IR spectra of NO dosed at RT (decreasing P_{NO} from 15 Torr (dotted line) spectrum to 10^{-3} Torr (dashed line) spectrum) on sample FeS50 activated at 773 K and subsequently treated for 1 h with O_2 at RT (a) and 573 K (b). The insets of parts (a) and (b) report the evolution of the spectra in the 2170–$1985\,cm^{-1}$ range where oxidation products are observed. (c) The $P_{NO} = 15$ Torr spectra obtained after re-activation in vacuo at 573 K (solid line), 773 K (dotted line) and 973 K (dashed line) of the sample oxidised at 573 K.

Fig. 5b reports the spectra obtained on the same sample previously oxidised with O_2 at 573 K. As the overall intensity of NO bands is reduced by a factor of ca. 8 it is inferred that after this treatment the capacity or iron species to adsorb NO is nearly completely inhibited. Also in this case the formation of oxidation products, absorbing in the 2150–2100 cm^{-1} range has been detected upon NO contact (see inset). These experiments indicate that O_2 at 573 K is adsorbed not only on clustered species but also on isolated Fe^{2+} species, and that the adsorbed oxygen is efficiently shielding the Fe centres.

To remove the adsorbed oxygen it is necessary to thermally activate the sample in vacuo at higher temperature. This is shown in Fig. 5c, where the NO spectra obtained on sample FeS50 re-activated in vacuo at 573–973 K after the oxidation treatment are shown. In fact, by increasing the re-activation temperature, the intensity of the nitrosylic bands is gradually recovered. However, only a treatment at 973 K is sufficient to restore the initial intensity of the nitrosylic bands. This indicates that the oxygen produced by dissociation of O_2 on isolated centres is strongly bonded.

4. Conclusions

Migration of Fe^{3+} from framework tetrahedral positions upon thermal treatments in vacuo leads to the formation of extraframework highly dispersed Fe^{2+} and Fe^{3+} species. A heterogeneous family of Fe^{2+} species has been detected by using NO as probe. These species can be classified in terms of their first shell environment, i.e. as $L_2N_nFe^{2+}$, where L are the framework SiO^- chemically linked groups and N are the framework oxygen atoms of the vicinal Si–O–Si bridges electrostatically linked. Depending upon the number of N ligands (i.e. upon the location on the zeolitic walls) the Fe^{2+} species can adsorb one, two, or three NO molecules with formation of well-defined nitrosylic species.

Two different Fe^{3+} extraframework species (giving rise to a doublet around 1900 cm^{-1}) are also detected. These species are reduced to highly coordinatively unsaturated Fe^{2+} species by prolonged activation in vacuo. The reduction process can be either due to spontaneous loss of oxygen or the action of carbonaceous impurities or both. Because of the low

concentration of Fe in most of the catalysts, the contribution of the latter reductive process cannot be excluded.

Coming to the oxidation experiments, only $L_2N_3Fe^{2+}$ species are able to adsorb O_2 at RT. This adsorption is supposed to occur on Fe^{2+} couples in dimeric or polymeric species, with formation of bridging $Fe^{3+}(O)^{2-}Fe^{3+}$ or $Fe^{3+}(O_2)^{2-}Fe^{3+}$ species. Higher interaction temperature (573 K) are needed to oxidise isolated L_2NFe^{2+} species. In this case the formation of FeO^{2+} species can be hypothesised. The adsorbed oxygen formed upon oxidation with O_2 at 573 K is strongly bonded, needing high temperature re-activation in vacuo (973 K) to be totally removed.

References

[1] R.L. Garten, W.N. Delgass, M. Boudart, J. Catal. 18 (1970) 90.
[2] K.-I. Segawa, Y. Chen, J.E. Kubsh, W.N. Delgass, J.A. Dumesic, W.K. Hall, J. Catal. 76 (1982) 112.
[3] J.W. Jermyn, T.J. Johnson, E.F. Vansant, J.H. Lunsford, J. Phys. Chem. 77 (1973) 2964.
[4] D. Ballivet-Tkatchenko, G. Coudurier, Inorg. Chem. 18 (1979) 558.
[5] T. Bein, P.A. Jacobs, J. Chem. Soc., Faraday Trans. 80 (1984) 1391.
[6] J.B. Nagy, M. Van Eeno, E.G. Derouane, J. Catal. 58 (1979) 230.
[7] K. Weissermehl, H.J. Arpe, Industrial Organic Chemistry, VCH, New York, 1993, p. 344.
[8] E. Suzuki, K. Nakashiro, Y. Ono, Chem. Lett. 9 (1988) 953.
[9] M. Gubelmann, J.M. Popa, P.J. Tirel, US Patent 5,055,623 (1991).
[10] A.S. Kharitonov, T.N.L. Alexandrova, A. Vostrikova, K.G. Ione, G.I. Panov, Russian Patent 4,445,646 (1988).
[11] G.I. Panov, V.I. Sobolev, K.A. Dubkov, V.N. Parmon, N.S. Ovanesyan, A.E. Shilov, A.A. Shteinman, React. Kinet. Catal. Lett. 61 (1997) 251.
[12] K.A. Dubkov, V.I. Sobolev, E.P. Talsi, M.A. Rodkin, N.H. Watkins, A.A. Shteinman, G.I. Panov, J. Mol. Catal. A 123 (1997) 155.

[13] J. Green, H. Dalton, Biochem. J. 259 (1989) 167.

[14] L. Shu, J.C. Neisheim, K. Kauffmann, E. Münck, J.D. Lipscomb, L. Que Jr., Science 275 (1997) 515.

[15] I.W.C.E. Arends, R.A. Sheldon, M. Wallau, U. Schuchardt, Angew. Chem. Int. Ed. Engl. 36 (1997) 1144.

[16] R. Szostak, T.L. Thomas, J. Catal. 100 (1986) 555.

[17] R. Szostak, V. Nair, T.L. Thomas, J. Chem. Soc., Faraday Trans. 1 83 (1987) 487.

[18] S. Bordiga, R. Buzzoni, F. Geobaldo, C. Lamberti, E. Giamello, A. Zecchina, G. Leofanti, G. Petrini, G. Tozzola, G. Vlaic, J. Catal. 158 (1996) 486.

[19] P. Fejes, J.B. Nagy, J. Halász, A. Oszkó, Appl. Catal. A 175 (1998) 89.

[20] P. Fejes, J.B. Nagy, K. Lázár, J. Halász, Appl. Catal. A 190 (2000) 117.

[21] A. Ribera, I.W.C.E. Arends, S. de Vries, J. Pérez-Ramírez, R.A. Sheldon, J. Catal. 195 (2000) 287.

[22] V.I. Sobolev, G.I. Panov, A.S. Kharitonov, V.N. Romannikov, A.M. Volodin, K.G. Ione, J. Catal. 139 (1993) 435.

[23] G.I. Panov, V.I. Sobolev, A.S. Kharitonov, J. Mol. Catal. 61 (1990) 85.

[24] V.I. Sobolev, G.I. Panov, A.S. Kharitonov, V.N. Romannikov, A.M. Volodin, Kinet. Catal. 34 (1993) 797.

[25] V.I. Sobolev, A.S. Kharitonov, Ye.A. Paukstis, G.I. Panov, J. Mol. Catal. 84 (1993) 117.

[26] M.J. Filatov, A.G. Pelmenschikov, G.M. Zhidomirov, J. Mol. Catal. 80 (1993) 243.

[27] K. Yoshizawa, Y. Shiota, T. Yamabe, J. Am. Chem. Soc. 121 (1999) 147.

[28] G.I. Panov, G.A. Sheveleva, A.S. Kharitonov, V.N. Romannikov, L.A. Vostrikova, Appl. Catal. A 82 (1992) 31.

[29] A.S. Kharitonov, G.A. Sheveleva, G.I. Panov, V.I. Sobolev, Ye.A. Paukshtis, V.N. Romannikov, Appl. Catal. A 98 (1993) 33.

[30] R. Szostak, V. Nair, T.L. Thomas, J. Chem. Soc., Faraday Trans. 1 83 (1987) 487.

[31] P. Ratnasamy, R. Kumar, Catal. Today 9 (1991) 329.

[32] S. Yuen, Y. Chen, J.E. Kubsh, J.A. Dumesic, N. Topsøe, H. Topsøe, J. Phys. Chem. 86 (1982) 3022.

[33] L.M. Aparicio, W.K. Hall, S. Fang, M.A. Ulla, W.S. Millman, J.A. Dumesic, J. Catal. 108 (1987) 233.

[34] L.J. Lobree, I.-C. Hwang, J.A. Reimer, A.T. Bell, J. Catal. 186 (1999) 233.

[35] H.-Y. Chen, El.-M. El-Malki, X. Wang, R.A. van Santen, W.M.H. Sachtler, J. Mol. Catal. A 162 (2000) 159.

[36] G. Spoto, A. Zecchina, G. Berlier, S. Bordiga, M.G. Clerici, L. Basini, J. Mol. Catal. A 158 (2000) 107.

[37] A. Meagher, V. Nair, R. Szostak, Zeolites 8 (1988) 3.

[38] K. Yogo, S. Tanaka, T. Ono, T. Mikami, E. Kikuchi, Micropor. Mater. 3 (1994) 39.

[39] G. Berlier, G. Spoto, S. Bordiga, G. Ricchiardi, P. Fisicaro, A. Zecchina, I. Rossetti, E. Selli, L. Forni, E. Giamello, C. Lamberti, J. Catal., submitted for publication.